

Supporting Information

A NIR fluorescent probe for the detection and visualization of hydrogen sulfide using aldehyde group assisted thiolysis of dinitrophenyl ether strategy

Ming Qian^{†‡}, Liuwei Zhang[‡], Zhongji Pu[‡], Jing Xia[‡], Lili Chen[‡], Ying Xia[‡], Hongyan Cui[‡],
Jingyun Wang^{†‡*}, Xiaojun Peng[†]

[†]State Key Laboratory of Fine Chemicals, Dalian University of Technology, 116024, Dalian, Liaoning, P. R. China

[‡]School of Life Science and Biotechnology, Dalian University of Technology, 116024, Dalian, Liaoning, P.R. China

List of contents

Scheme S1 The synthesis procedure of intermediates.

Table S1 A comparison of NIR fluorescent probes for H₂S.

Table S2 The photophysical properties of **NDCM-CHO-OH** in different co-solvents.

Figure S1 The optical spectra of **NDCM-OH** and **NDCM-CHO-OH**.

Figure S2 The optical spectra of **NDCM-CHO-OH** and **NDCM-OH** in different solvents.

Figure S3 The fluorescence spectra for the verification of the reaction product.

Figure S4 The absorption response behavior of **NDCM-2** toward H₂S.

Figure S5 The fluorescence response of probe **NDCM-2** (10 μM) toward different concentrations of H₂S.

Figure S6 The HRMS for the verification of the sensing mechanism.

Figure S7 ¹H NMR for the verification of the sensing mechanism.

Figure S8 The selectivity of **NDCM-2** toward H₂S over various biological related analytes.

Figure S9 The selectivity of **NDCM-2** toward H₂S over biothiols.

Figure S10 Density functional theory (DFT) calculation of **NDCM-1** and **NDCM-OH**.

Figure S11 Effect of pH on **NDCM-2** and its sensing performance toward H₂S.

Figure S12 Photobleaching curves of **NDCM-2**.

Figure S13 Evaluating the preservation stability of probe **NDCM-2**.

Figure S14 Cytotoxicity of the probe **NDCM-2** on HeLa cells.

Figure S15 The confocal fluorescence imaging of the basal H₂S in four different cells.

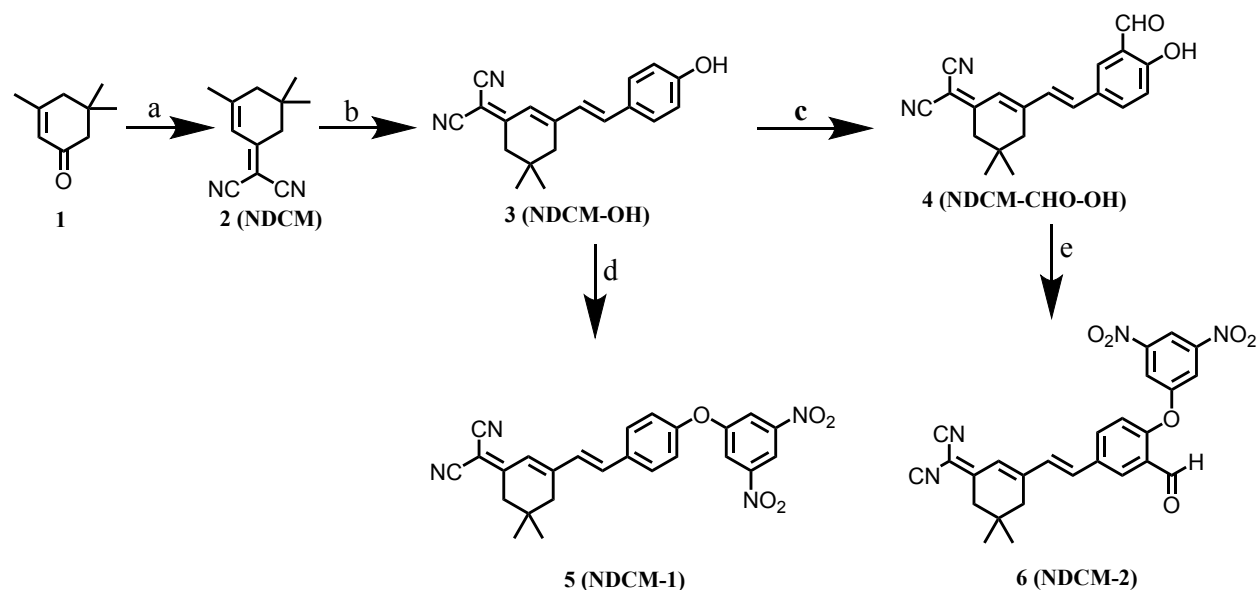
Figure S16 The co-staining experiment of **NDCM-2** with Hoechst 33342.

Figure S17 The co-staining experiment of **NDCM-2** with Lyso tracker red.

Figure S18 Fluorescence images of **NDCM-2** against different concentration of exogenous H₂S

Figure S19 Evaluating the photostability of **NDCM-2** in the sensing process against H₂S in living HeLa cells.

Figure S20- Figure S34 Structure verification of the synthesized compound by MS and NMR.



Scheme S1. The synthetic route of the probe. Reaction conditions: (a) malononitrile, piperidine, glacial acetic acid, EtOH, reflux, N₂ protection; (b) p-hydroxybenzaldehyde, piperidine, acetonitrile, reflux, N₂ protection; (c) Hexamethylenetetramine, trifluoroacetic acid, reflux; (d) DIEPA, 2,4-dinitrofluorobenzene, dry CH₂Cl₂, room temperature. (e) DIEPA, 2,4-dinitrofluorobenzene, dry CH₂Cl₂, room temperature.

The synthesis of NDCM

Isophorone (2.3 g, 16.7 mmol), malononitrile (1.32 g, 20.0 mmol), piperidine (0.2 mL, 2.0 mmol) and glacial acetic acid (0.10 g, 1.6 mmol) were dissolved in 100 mL EtOH, Then, the mixture was refluxed for 6 h under argon atmosphere. After the solvent was removed, the residue was dissolved with CH₂Cl₂, washed with water, and dried over Na₂SO₄. Finally, the solvent was evaporated under reduced pressure, and the crude product was purified by silica column chromatography (petroleum/dichloromethane = 1:2, v/v) to give a white solid (2.1 g, 67.7%). ¹H NMR (400 MHz, DMSO): δ 6.56 (d, J = 1.2 Hz, 1H), 2.53 (s, 2H), 2.23 (s, 2H), 2.05 (s, 3H), 0.95 (s, 6H). ¹³C NMR (126 MHz, DMSO): 171.28, 162.37, 119.38, 113.42, 112.63, 76.08, 44.69, 41.71, 31.87, 27.04, 24.99. HRMS: calculated for [M-H]⁻: 185.1079; found: 185.1089.

The synthesis of NDCM-OH

NDCM (1 g, 5.4 mmol), p-hydroxybenzaldehyde (732 mg, 6.0 mmol), five drops of piperidine were dissolved in 40 mL anhydrous acetonitrile. The mixture was refluxed for 5 h under argon atmosphere. Subsequently, the solvent was removed under reduced pressure. The resulting residue

was dissolved in 20 mL dichloromethane, washed with water for three times, and dried over anhydrous Na₂SO₄. After the removal of the solvent, the crude product was purified by silica column chromatography (dichloromethane: acetic ether = 100:1) to afford the **NDCM-OH** as a red solid (1.17 g, 75%). ¹H NMR (400 MHz, DMSO): δ 9.98 (s, 1H), 7.55 (d, J = 8.7 Hz, 2H), 7.29 – 7.14 (m, 2H), 6.83 ~ 6.76 (m, 3H), 2.59 (s, 2H), 2.53 (s, 2H), 1.01 (s, 6H). ¹³C NMR (126 MHz, DMSO): δ 170.23, 159.31, 156.67, 138.25, 129.83, 127.10, 126.22, 121.34, 115.85, 114.09, 113.27, 74.79, 42.31, 38.19, 31.62, 27.41. HRMS: calculated for [M-H]⁻: 289.1341; found: 289.1351

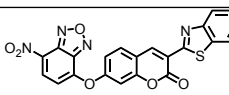
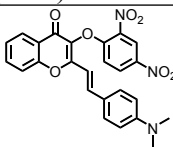
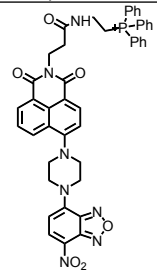
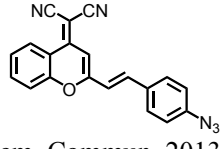
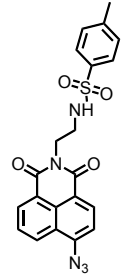
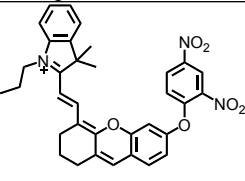
The synthesis of **NDCM-CHO-OH**

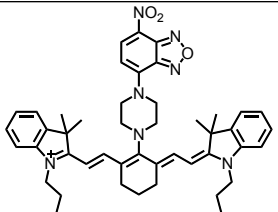
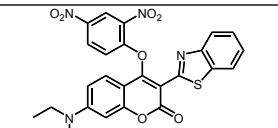
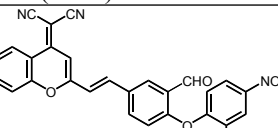
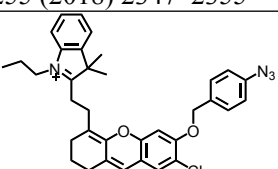
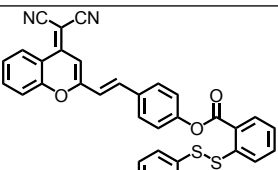
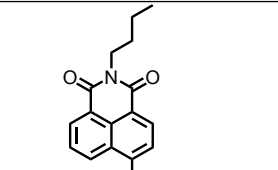
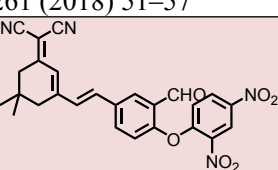
Hexamethylenetetramine (168 mg, 1.2 mmol) was added to solution of **NDCM-OH** (290.0 mg, 1.0 mmol) in trifluoroacetic acid (10 mL). The mixture was refluxed for 5 h. After complete reaction, the solvent was evaporated under a rotary evaporator, diluted with water and then neutralized with NaOH until the pH reached 7.0. Subsequently, the solution was extracted with dichloromethane. The organic layer was washed with water for three times, dried over anhydrous sodium sulfate. The crude product was purified by silica gel column chromatography with dichloromethane as the eluent to afford **NDCM-CHO-OH** as a yellow solid (116.6 mg, 43%). ¹H NMR (400 MHz, DMSO): δ 11.15 (s, 1H), 10.29 (s, 1H), 7.97 (d, J = 2.2 Hz, 1H), 7.89 (dd, J = 8.7, 2.2 Hz, 1H), 7.37 ~ 7.25 (m, 2H), 7.04 (d, J = 8.6 Hz, 1H), 6.88 (s, 1H), 2.61 (s, 2H), 2.53 (s, 2H), 1.01 (s, 6H). ¹³C NMR (126 MHz, DMSO): δ 190.63, 170.27, 161.87, 156.09, 136.69, 134.96, 128.75, 127.96, 127.64, 122.62, 122.19, 118.08, 113.92, 113.08, 75.75, 42.27, 38.14, 31.62, 27.41. HRMS: calculated for [M-H]⁻: 317.1290; found: 317.1293.

The synthesis of **NDCM-1**

The control compound **NDCM-1** was synthesized according to the similar synthesis procedure of **NDCM-2** using **NDCM-OH** as the reactant. ¹H NMR (500 MHz, DMSO-d₆): δ 10.18 (s, 1H), 8.93 (d, J = 2.7 Hz, 1H), 8.47 (dd, J = 9.2, 2.8 Hz, 1H), 8.30 (d, J = 1.9 Hz, 1H), 8.10 (dd, J = 8.6, 1.9 Hz, 1H), 7.57 (d, J = 16.2 Hz, 1H), 7.46~7.29 (m, 3H), 6.96 (s, 1H), 2.63 (s, 2H), 2.55 (s, 2H), 1.02 (s, 6H). ¹³C NMR (DMSO-d₆): δ 170.26, 155.57, 154.64, 154.33, 141.77, 139.68, 136.08, 133.91, 130.05, 129.97, 129.65, 123.03, 121.89, 120.40, 120.06, 113.76, 112.95, 76.54, 42.28, 38.17, 31.65, 27.41. HRMS: calculated for [M-H]⁻: 455.1356; found: 455.1368.

Table S1. A comparison of NIR fluorescent probes for H₂S.

Probe	Properties	Stokes shift	Fluorescence enhancement	Response time	Detection limit	Applications
 Analytica Chimica Acta 896 (2015) 128-136	Abs: 450 nm Em 490 nm Two-photon	40 nm	35-fold	2 min	120 nM	Cells and tissues
 Sensors and Actuators B 221 (2015) 951-955	Abs: 450 nm Em: 612 nm	162 nm	112-fold	30 min	90 nM	Cells
 Anal. Chem. 2016, 88, 5476-5481	Abs: 394/520 nm Em 532 nm Mitochondria-Targeted	138 nm	68-fold	40 min	2.46 μM	Cells
 Chem. Commun. 2013, 49, 3890-3892.	Abs :520 nm Em:670 nm NIR emission	150 nm	65-fold	60 min	3.05 μM	Cells
 Sci. Rep. 2017, 7, 12944.	Abs :440 nm Em:545 nm ER Targeted	105 nm	45-fold	30 min	7.77 μM	Cells, tissues and zebrafish
 Sci. Rep. 2016, 6, 18868.	Abs :670 nm Em:723 nm NIR excitation and emission	53 nm	50-fold	20 min	38 nM	Cells and mice

 Chem. Sci. 2017, 8, 2776–2781.	Abs: 740 nm Em: 796 nm NIR excitation and emission	56 nm	87-fold	30 min	39.6 nM	Cells and mice
 Sensors and Actuators B 232 (2016) 705–711	Abs: 370 nm Em: 424 nm	54 nm	200-fold	180 min	90 nM	Cells
 Sensors and Actuators B 255 (2018) 2347–2355	Abs: 518 nm Em: 655 nm NIR emission	137 nm	32-fold	8 min	83 nM	Cells
 Biosens. Bioelectron. 2017, 89, 919–926.	Abs: 680 nm Em: 720 nm NIR excitation and emission	40 nm	20-fold	30 min	260 nM	Cells and mice
 Dyes Pigm. 2018, 153, 206–212.	Abs: 560 nm Em: 680 nm NIR emission	130 nm	About 25-fold	30 min	1.1 nM	Cells
 Sensors and Actuators B 261 (2018) 51–57	Abs: 452 nm Em: 552 nm Two photon Ratio metric detection	100 nm	Not mentioned	5 min	0.24 μM	Cells
 This work	Abs: 490 nm Em: 660 nm NIR emission	170 nm	160-fold	15 min	58.797 nM	Cells, tissues and mice

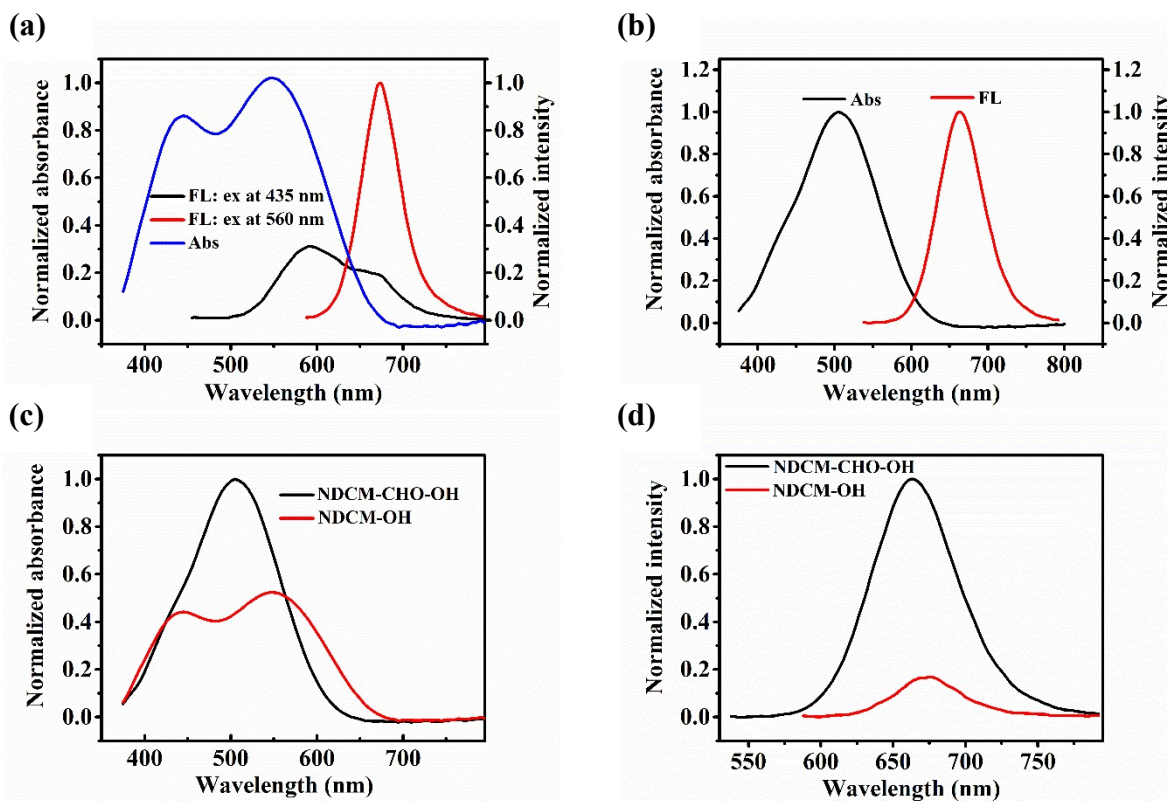


Figure S1. The spectra of **NDCM-OH** and **NDCM-CHO-OH** in PBS-DMSO solution (pH=7.4, 1:1). (a) The normalized spectra of **NDCM-OH**. (b) The normalized spectra of **NDCM-CHO-OH**. (c) Comparison of two fluorophores in absorbance. (d) Comparison of two fluorophores in fluorescence emission.

Table S2. The photophysical properties of fluorophore **NDCM-CHO-OH** in different co-solvents (PBS solution with addition of 50% organic solvents).

solvents	λ_{\max} (nm)	ϵ_{\max} ($\times 10^4$)	λ_{em} (nm)	Φ	δ shift(nm)
CH₃CN	490	4.01	660	0.233777	170
DMSO	505	4.53	664	0.381135	159
Acetone	505	4.38	664	0.157977	159
DMF	510	4.72	664	0.368865	154
CH₃OH	485	4.32	652	0.200058	167
THF	525	4.19	666	0.233269	141
1,4-Dioxane	505	4.45	662	0.279373	157
EtOH	500	4.74	658	0.215895	158

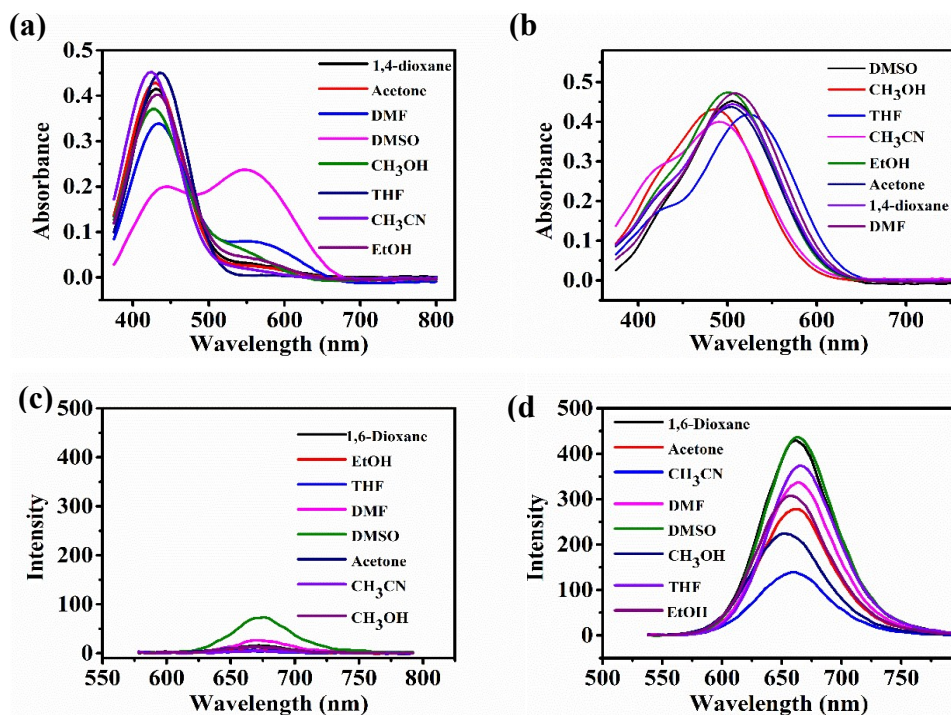


Figure S2. The optical spectra of fluorophore **NDCM-CHO-OH** and **NDCM-OH** in different co-solvents (PBS solution with addition of 50% organic solvents). (a) The absorption spectrum of **NDCM-OH** in different co-solvents. (b) The absorption spectrum of **NDCM-CHO-OH** in different co-solvents. (c) The fluorescence spectrum of **NDCM-OH** in different co-solvents. (d) The fluorescence spectrum of **NDCM-CHO-OH** in different co-solvents.

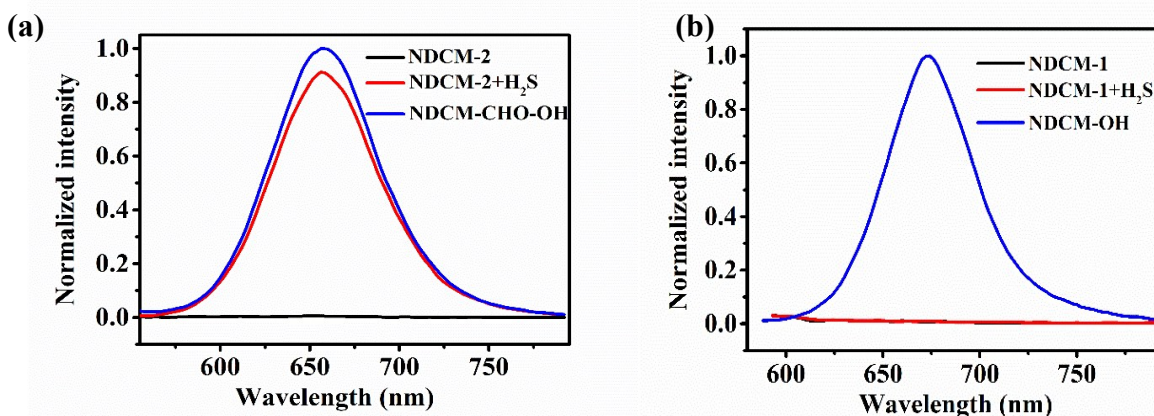


Figure S3. The spectra for the verification of the reaction product. (a) The fluorescence spectra of **NDCM-2** (10 μ M), **NDCM-2** (10 μ M) + 100 μ M Na₂S and **NDCM-CHO-OH** (10 μ M) in PBS-CH₃CN solution (pH 7.4, 1:1), excitation wavelength: 490 nm. (b) The fluorescence spectra of **NDCM-1** (10 μ M), **NDCM-1** (10 μ M) + 100 μ M Na₂S and **NDCM-OH** (10 μ M) in PBS-CH₃CN solution (pH 7.4, 1:1), excitation wavelength: 490 nm.

μM) + $100 \mu\text{M Na}_2\text{S}$ and **NDCM-OH** ($10 \mu\text{M}$) in PBS-DMSO solution (pH 7.4, 1:1), excitation wavelength: 560 nm.

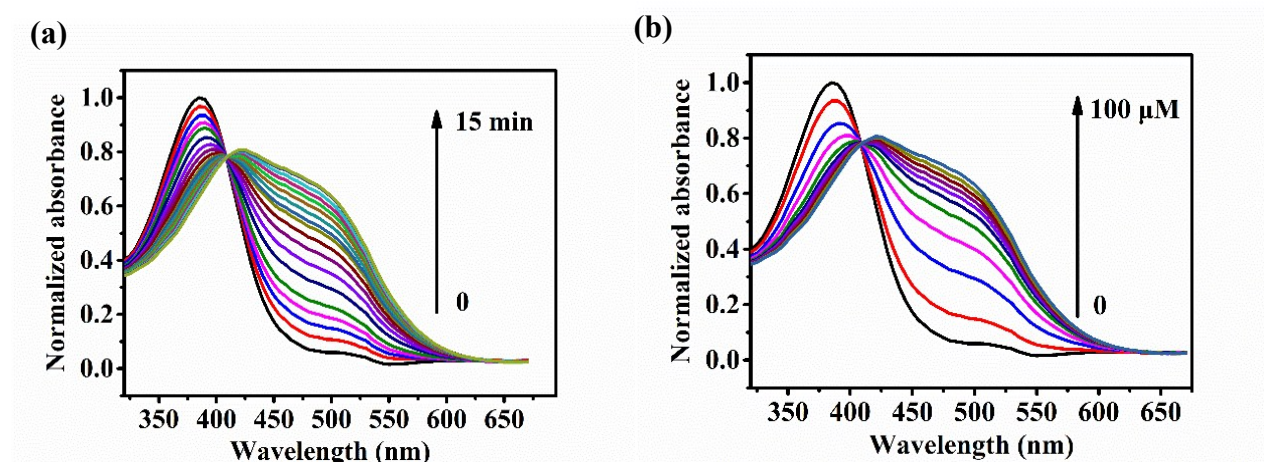


Figure S4. The absorption response behavior toward H_2S in PBS- CH_3CN solution (pH=7.4, 1:1). (a) The time-dependent normalized absorption spectra change in 15 min upon the addition of $100 \mu\text{M Na}_2\text{S}$. (b) The normalized absorption spectra change of **NDCM-2** toward different Na_2S concentration (0, 10, 20, 30, 40, 50, 60, 70, 80, 90, $100 \mu\text{M}$) for 15 min. Excitation wavelength: 490 nm.

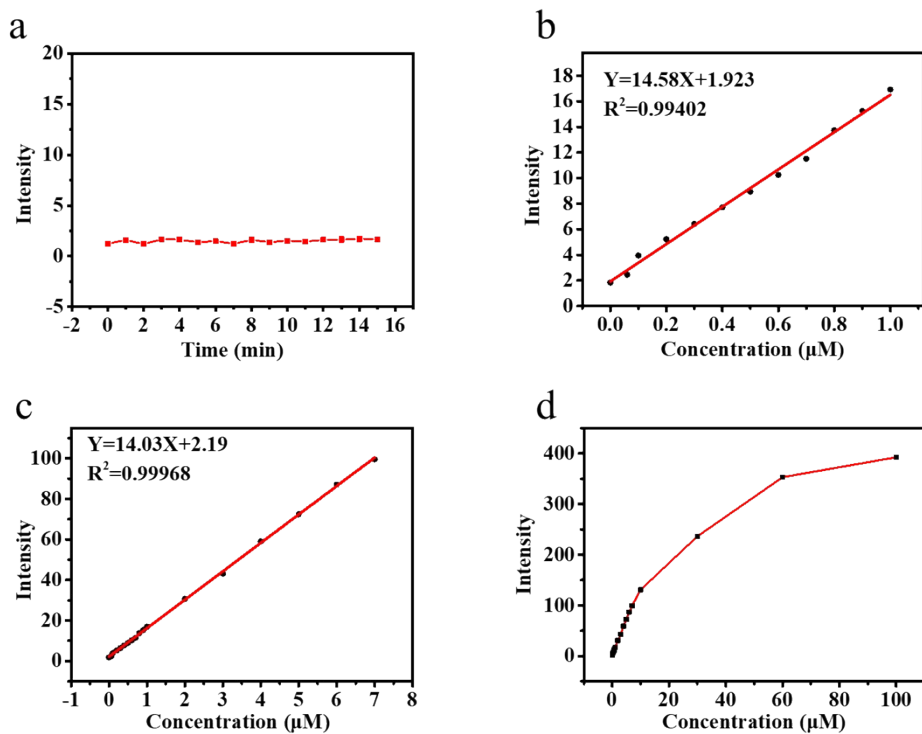


Figure S5. Fluorescence response of probe **NDCM-2** (10 μM) toward different concentrations of Na_2S . (a) The time-dependent fluorescence intensity (660 nm) change of **NDCM-2** without the addition of Na_2S . (b) The linear relationship between the fluorescence intensity (660 nm) and extremely low Na_2S concentration (0, 0.06, 0.1, 0.2, 0.3, 0.4, 0.5, 0.6, 0.7, 0.8, 0.9, 1 μM). (c) The linear relationship between the fluorescence intensity (660 nm) and low Na_2S concentration (0, 0.06, 0.1, 0.2, 0.3, 0.4, 0.5, 0.6, 0.7, 0.8, 0.9, 1, 2, 3, 4, 5, 6, 7 μM). (d) The fluorescence intensity (660 nm) change of **NDCM-2** toward various Na_2S concentration (0, 0.06, 0.1, 0.2, 0.3, 0.4, 0.5, 0.6, 0.7, 0.8, 0.9, 1, 2, 3, 4, 5, 6, 7, 10, 30, 60, 100 μM). Excitation wavelength: 490 nm.

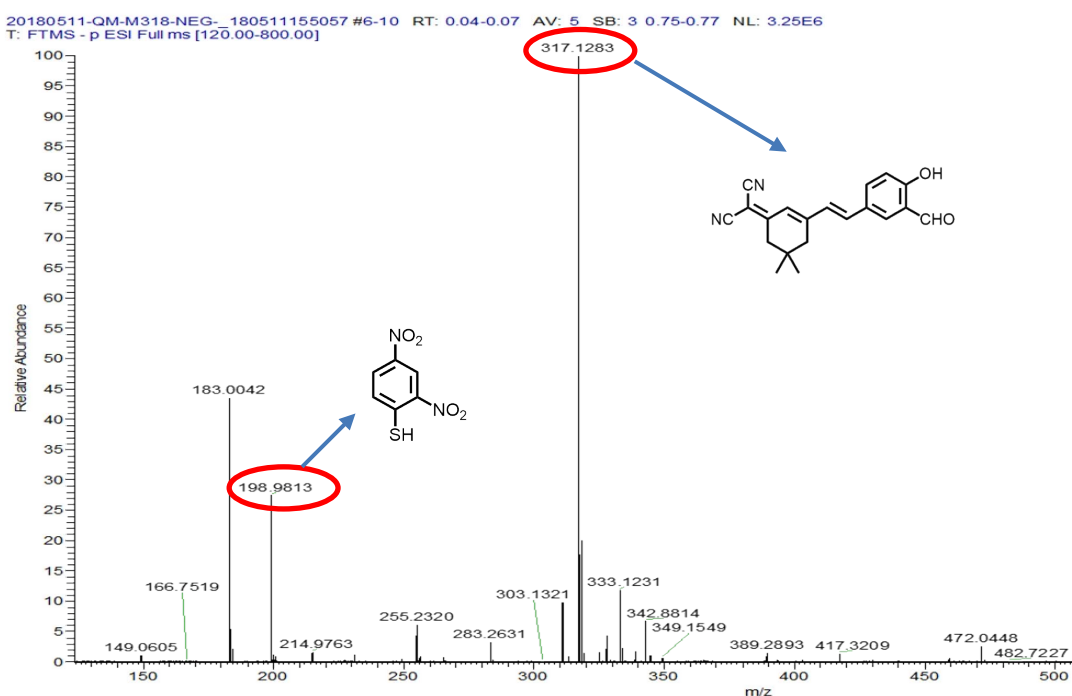


Figure S6. Verifying the sensing mechanism of **NDCM-2** toward H_2S by HRMS.

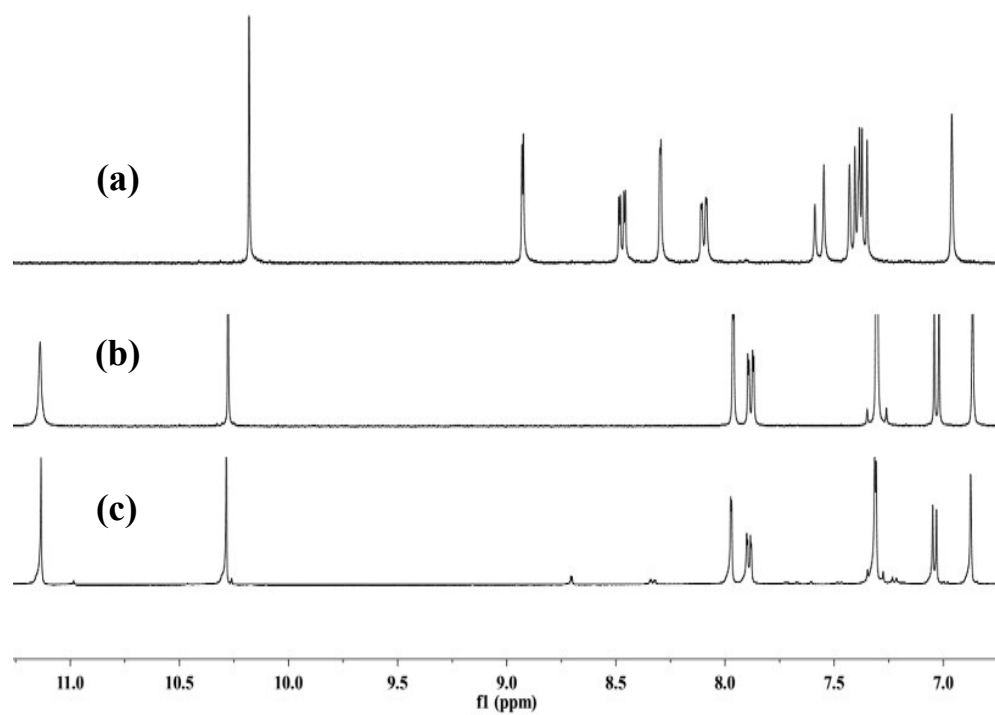


Figure S7. ¹H NMR for the verification of the sensing mechanism. (a) ¹H NMR spectra (δ 6.5~11.5) of **NDCM-2**. (b) The fluorophore **NDCM-CHO-OH**. (c) The isolated product of **NDCM-2** + Na₂S.

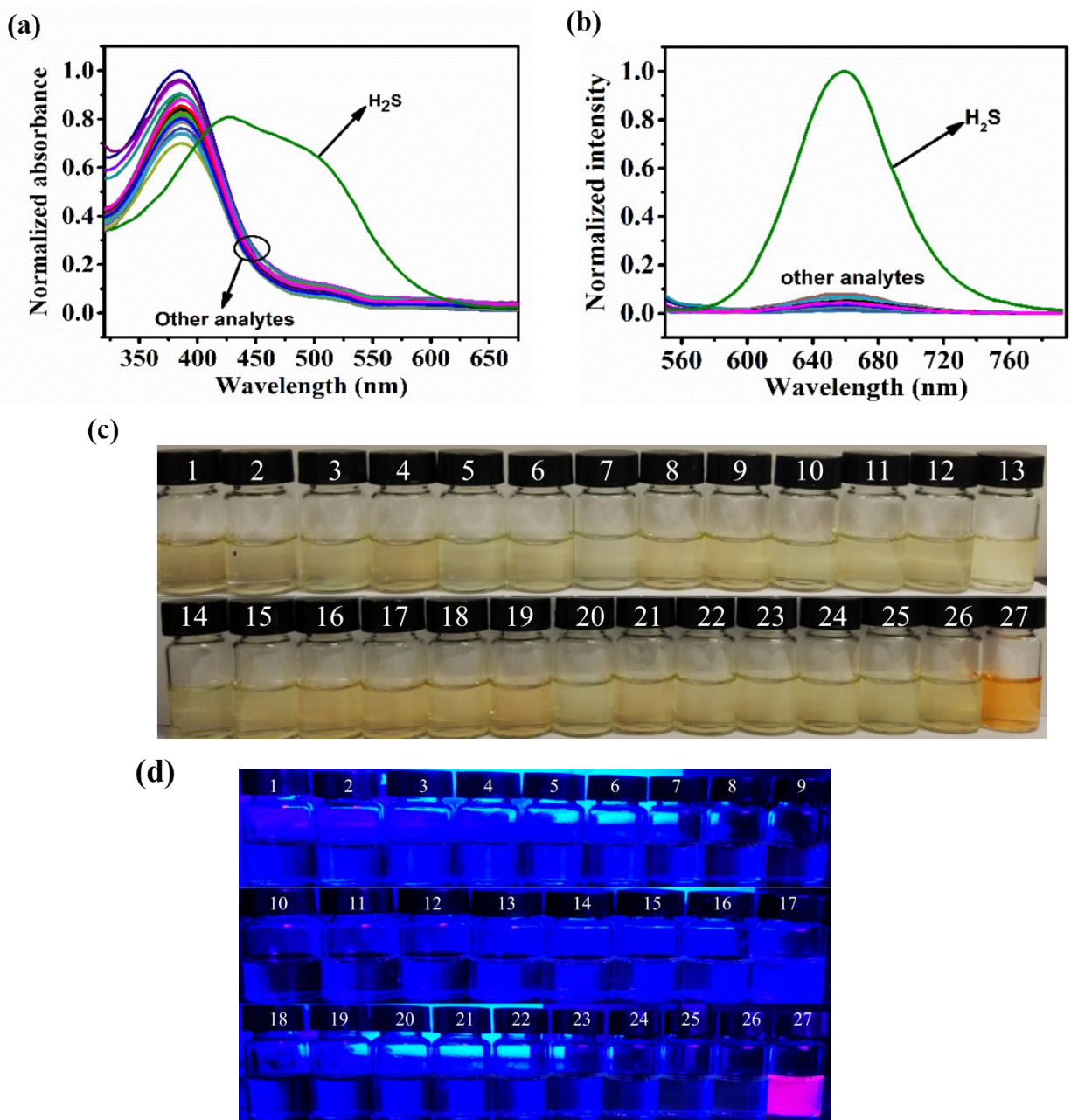


Figure S8. The selectivity of **NDCM-2** toward H_2S over various biological related analytes. (a) Absorption spectra change of **NDCM-2** ($10\ \mu\text{M}$) toward various analytes (Na_2S : $100\ \mu\text{M}$, other analytes: $1\ \text{mM}$) in PBS- CH_3CN solution (pH 7.4, 1:1). (b) Fluorescence spectra change of probe **NDCM-2** ($10\ \mu\text{M}$) toward various analytes (Na_2S : $100\ \mu\text{M}$, other analytes: $1\ \text{mM}$) in PBS- CH_3CN solution (pH 7.4, 1:1). (c) Color changes of probe **NDCM-2** ($10\ \mu\text{M}$) upon the addition of various analytes ($100\ \mu\text{M}$ for Na_2S and $1\ \text{mM}$ for other analytes) under bright field. (d) Fluorescence color changes of probe **NDCM-2** ($10\ \mu\text{M}$) upon the addition of various analytes ($100\ \mu\text{M}$ for Na_2S and $1\ \text{mM}$ for other analytes) under a $365\ \text{nm}$ UV-lamp. 1:

HCO₃⁻, 2: HPO₄⁻, 3: Glucose, 4: Zn²⁺, 5: AcO⁻, 6: Ni²⁺, 7: Cl⁻, 8: N₃⁻, 9: I⁻, 10: S₂O₃²⁻, 11: Citrate, 12: SO₄²⁻, 13: NO₃⁻, 14: S₂O₇²⁻, 15: SO₃²⁻, 16: Pro, 17: Met, 18: Val, 19: Leu, 20: Ser, 21: Glu, 22: Ala, 23: Cys, 24: GSH, 25: Hcy, 26: H₂O₂, 27: Na₂S. Excitation wavelength: 490 nm.

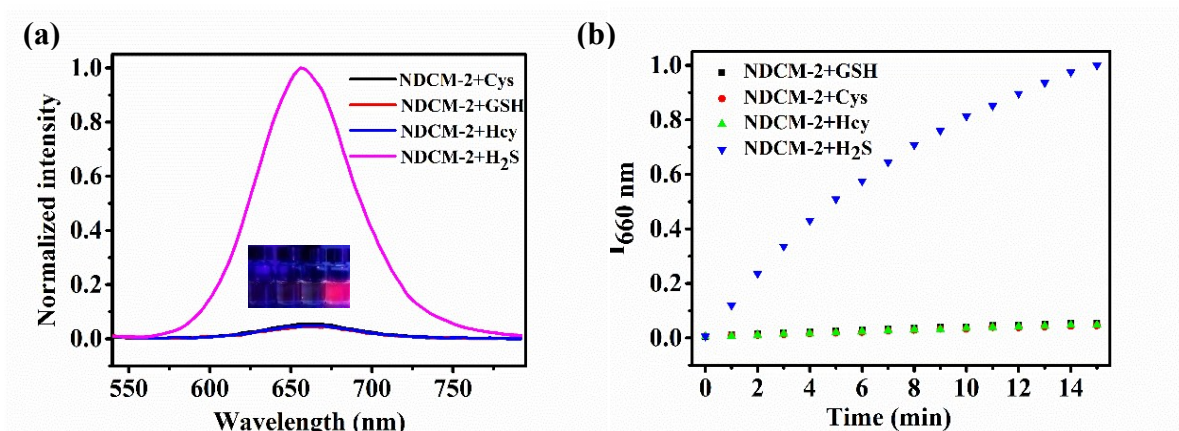


Figure S9. The selectivity of **NDCM-2** toward H₂S over biothiols (GSH, Hcy, Cys) in PBS-CH₃CN solution (pH=7.4, 1:1). (a) The normalized fluorescence spectra change of **NDCM-2** upon addition of Na₂S (100 μM) and three biothiols (100 μM), inset: the color change of **NDCM-2** toward Na₂S and three biothiols under UV Lamp (365 nm). (b) The normalized fluorescence intensity at 660 nm changed with time upon addition of 100 μM Na₂S and 100 μM GSH, Hcy, Cys. The excitation wavelength: 490 nm.

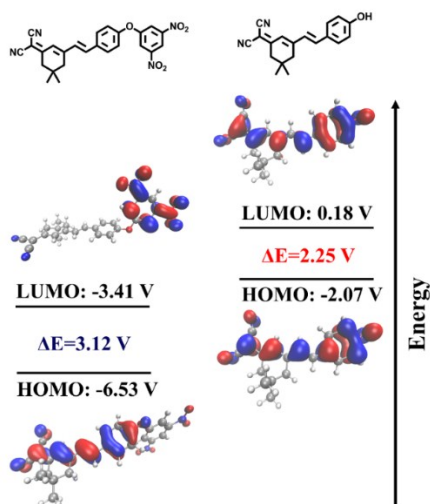


Figure S10. Density functional theory (DFT) optimized structures and frontier molecular orbitals (MOs) of **NDCM-1** and **NDCM-OH**. The calculations were obtained by DFT at the B3LYP/6-311G (d, p)/level using Gaussian 16 program.

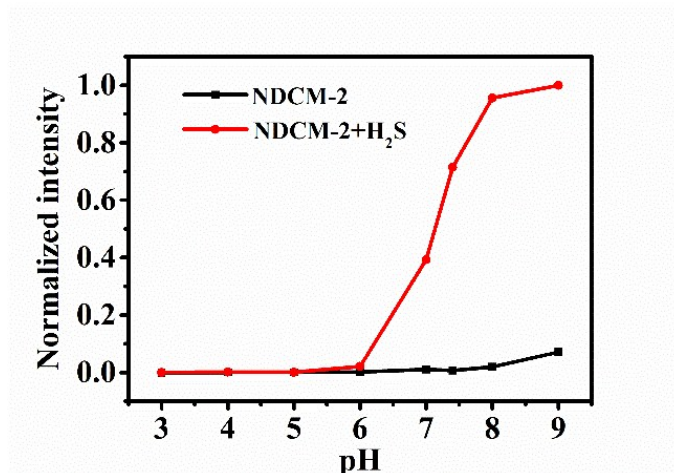


Figure S11. Fluorescence intensity of probe **NDCM-2** (10 μM) at 660 nm under different pH values (from 3.0 to 9.0) in the absence and presence of Na_2S (100 μM). Excitation wavelength: 490 nm.

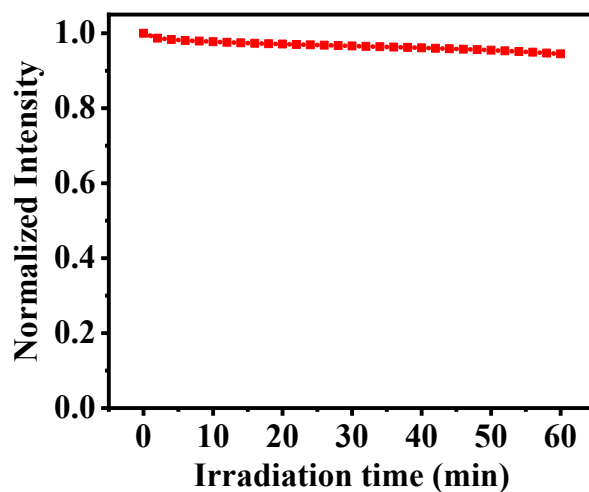


Figure S12. Photobleaching curves for the final reaction solution of **NDCM-2** and 100 μM H_2S exposed to the light irradiation under the high voltage mode (800 V) of fluorescence spectrophotometer.

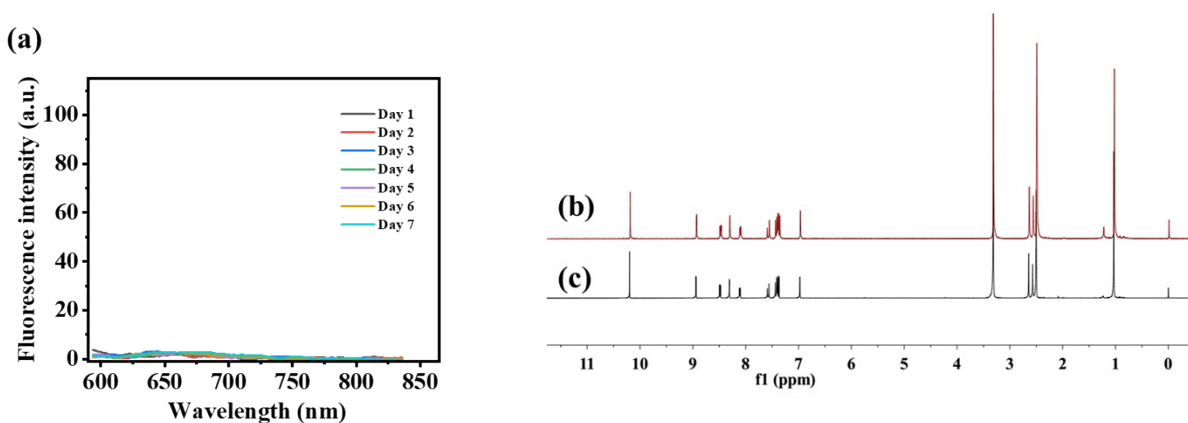


Figure S13. Evaluating the preservation stability of probe **NDCM-2**. (a) Fluorescence spectra change of the stock solution of probe **NDCM-2** (10 μM) in the preservation time period of 0-7 days. Excitation wavelength: 490 nm. (b-c) The NMR spectra comparison of **NDCM-2** before and after preservation for four months. The spectrum of (c) was measured after the preservation of pure **NDCM-2** solid in refrigerator for four months.

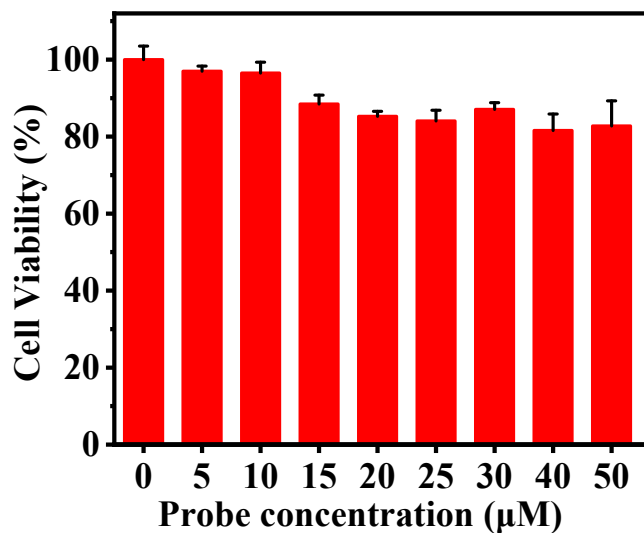


Figure S14. Cytotoxicity of the probe **NDCM-2** against HeLa cells evaluated by a standard MTT assay, the data are presented as mean \pm S.D.

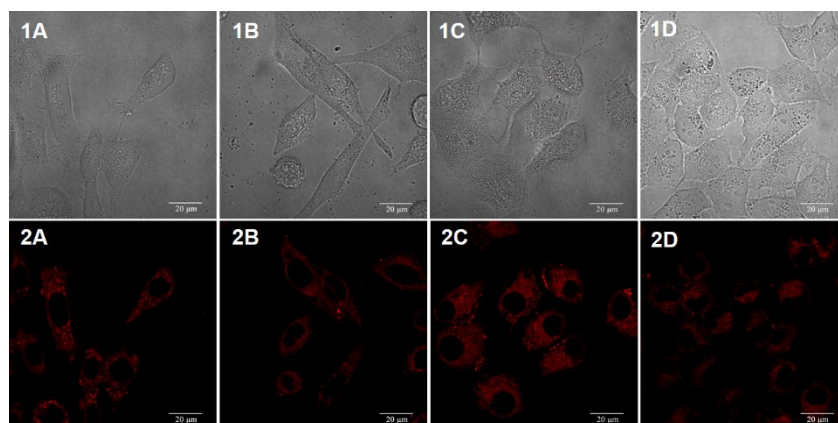


Figure S15. The confocal fluorescence imaging of the basal H_2S in four different cells using probe **NDCM-2** ($10 \mu M$). (2A) COS-7 cells. (2B) MCF-7 cells. (2C) HepG-2 cells. (2D) HeLa cells. 1A, 1B, 1C, and 1D are the corresponding bright-field image of 2A, 2B, 2C, and 2D. The fluorescence images were obtained by collecting the emissions ranging from 620 to 720 nm upon excitation at 488 nm. Scar bar= $20 \mu m$.

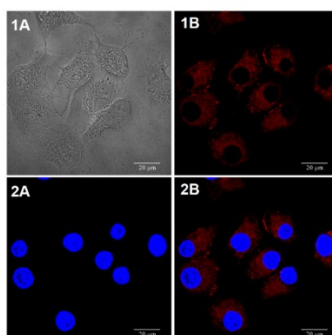


Figure S16. The co-staining experiments of **NDCM-2** ($10 \mu M$) in HepG-2 cells using Hoechst 33342 as the nucleus staining dyes. (1A): Bright field. (1B): Fluorescence imaging of basal H_2S using **NDCM-2**. (2A): Fluorescence imaging of Hoechst 33342. (2B): Merge of (1B) and (2A). Excitation wavelength: 405 nm for Hoechst 33342 and 488 nm for **NDCM-2**. The fluorescence images of **NDCM-2** were obtained by collecting the emissions at 620-720 nm upon excitation at 488 nm and the fluorescence images of Hoechst 33342 were obtained by collecting the emissions at 420-520 nm. Scar bar= $20 \mu m$.

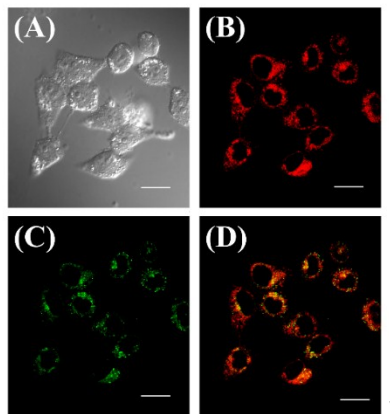


Figure S17 The co-staining experiments of **NDCM-2** (10 μM) in HeLa cells using Lyso-tracker red as the specific lysosome staining dyes. (A): Bright field. (B): Fluorescence images of **NDCM-2** against 100 μM exogenous H_2S . (C): Fluorescence images of Lyso-tracker red. (D): Merge of (B) and (C). Excitation wavelength: 559 nm for Lyso-tracker red and 488 nm for **NDCM-2**. The fluorescence images of **NDCM-2** and Lyso tracker red were obtained by collecting the emissions at 620-720 nm and 560-600 nm with confocal laser scanning microscopy (Olympus, FV1000-IX81), respectively. Scar bar=20 μm .

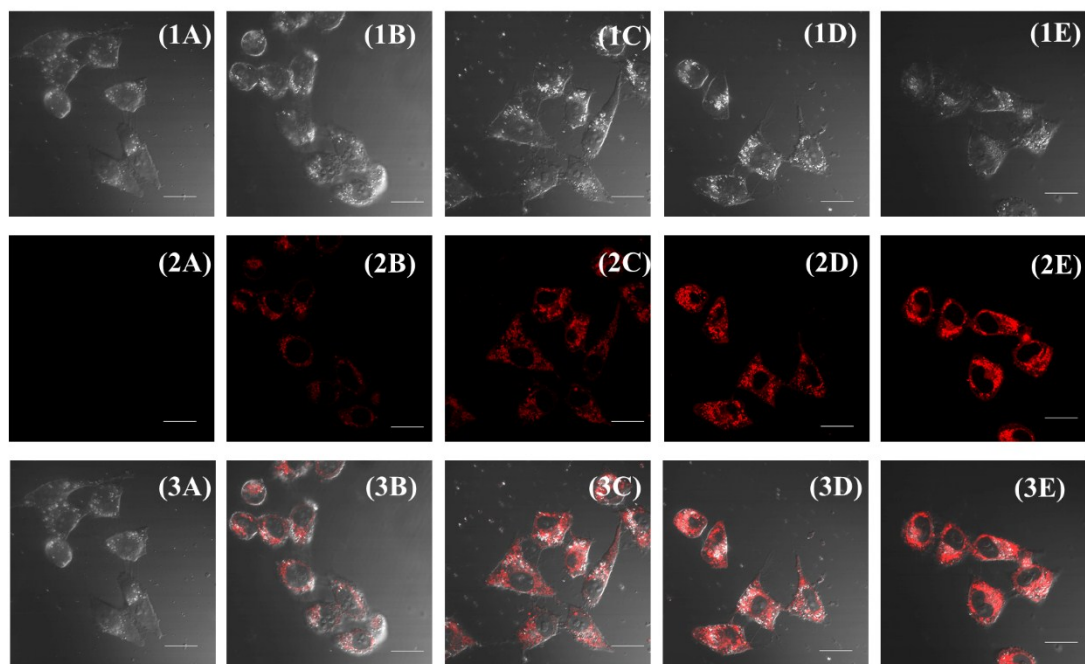


Figure S18. Fluorescence images of **NDCM-2** against different concentration of exogenous H_2S (0, 2 μM , 20 μM , 50 μM , 100 μM) in living HeLa cells. (2A): PPG (1 mM) pre-treated cells were incubated with 10 μM **NDCM-2** for 30 min only. (2B-2E): PPG (1 mM) pre-treated cells were incubated with 5 μM , 20 μM ,

50 μM , 100 μM Na_2S for 30 min respectively, then incubated with 10 μM **NDCM-2** for 30 min. (1A-1E) and (3A-3E) are the corresponding bright field and merge field of (2A-2E), respectively. The fluorescence images were obtained by collecting the emissions at 620-720 nm under the excitation wavelength of 488 nm with confocal laser scanning microscopy (Olympus, FV1000-IX81). Scar bar=20 μm .

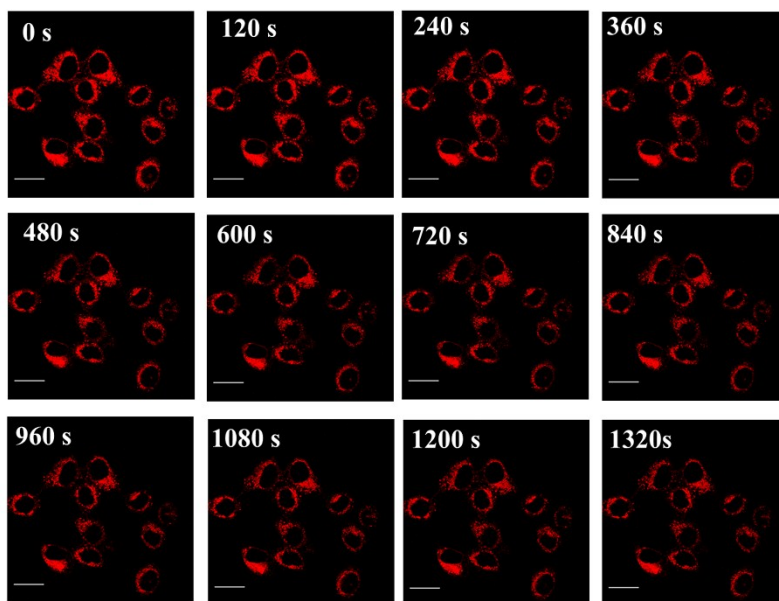


Figure S19. Evaluating the photostability of probe **NDCM-2** in the sensing process against H_2S in living HeLa cells. The cells were incubated with 100 μM H_2S at 37 $^\circ\text{C}$ for 30 min, followed by the incubation of 10 μM **NDCM-2** for 30 min at 37 $^\circ\text{C}$. Images were taken by confocal fluorescent microscopy (Olympus, FV1000-IX81) for different times (0, 120s, 240s, 360s, 480s, 600s, 720s, 840s, 960s, 1080s, 1200s, 1320s) with the excitation at 488 nm and the emission collection range from 620 to 700 nm. Scale bar=20 μm .

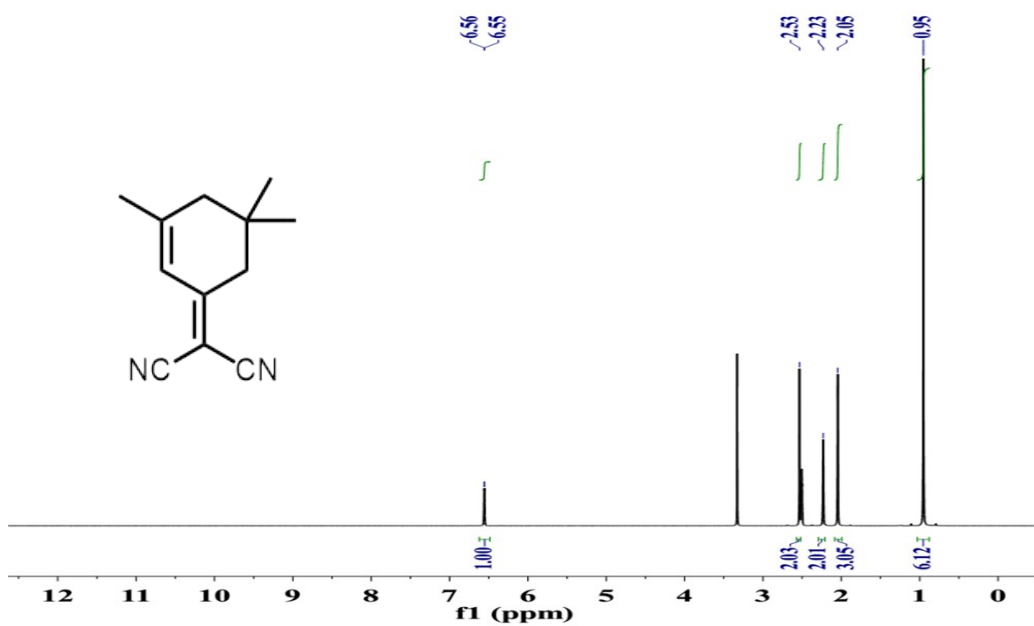


Figure S20. ¹H NMR spectra of NDCM in DMSO-d₆

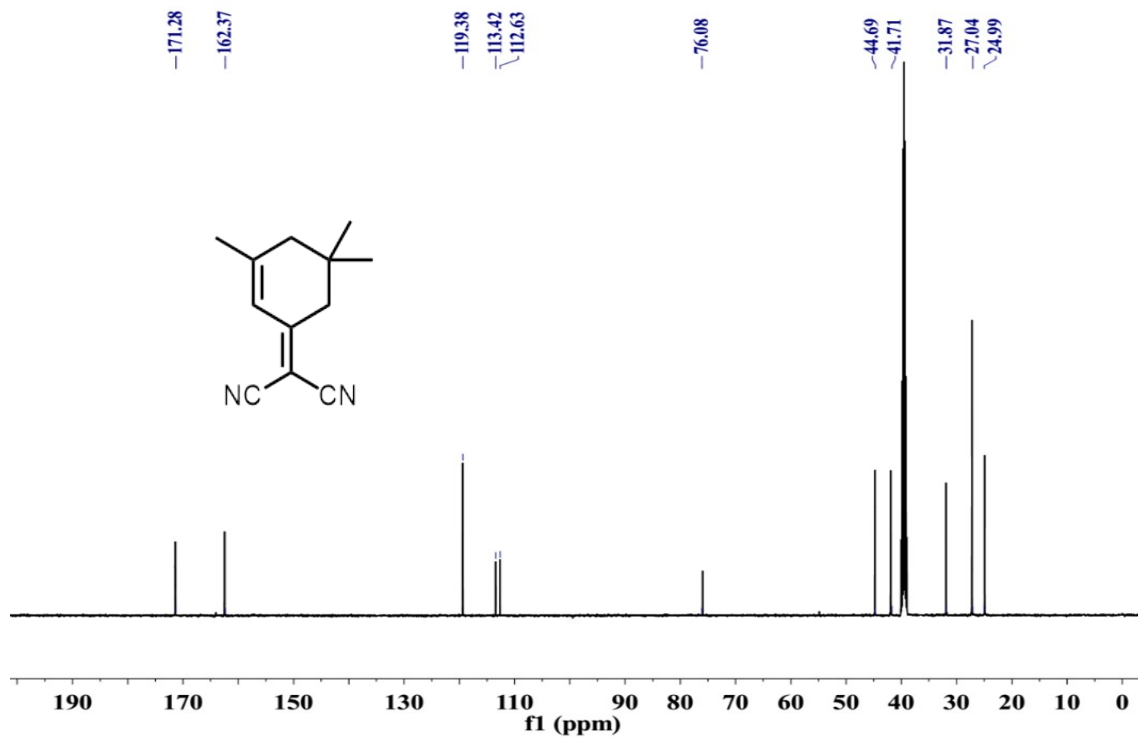


Figure S21. ¹³C NMR spectra of NDCM in DMSO-d₆

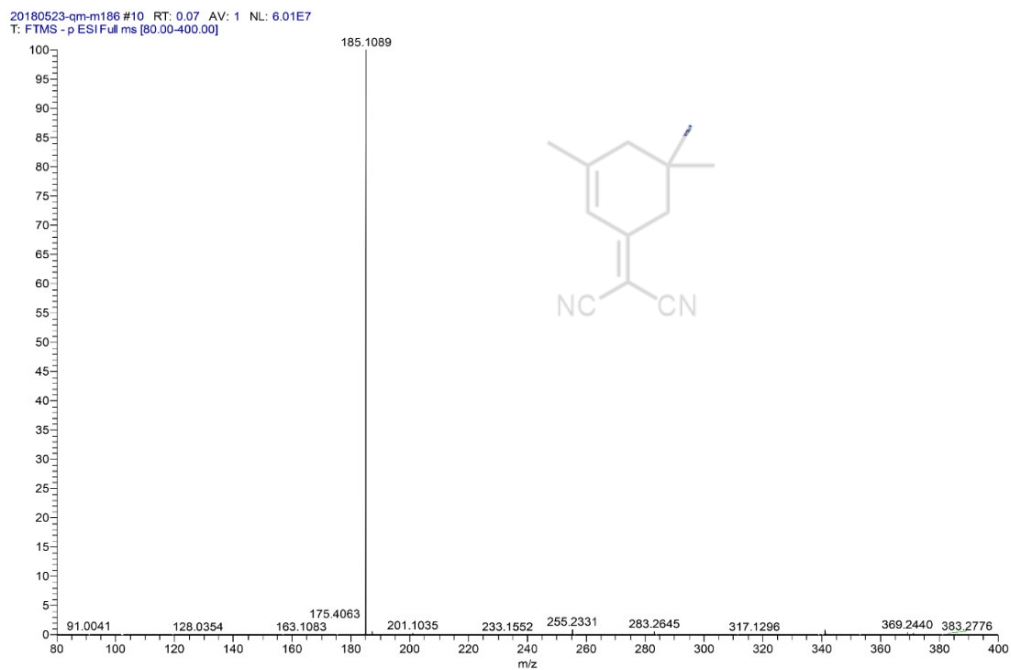


Figure S22. HRMS spectra of NDCM

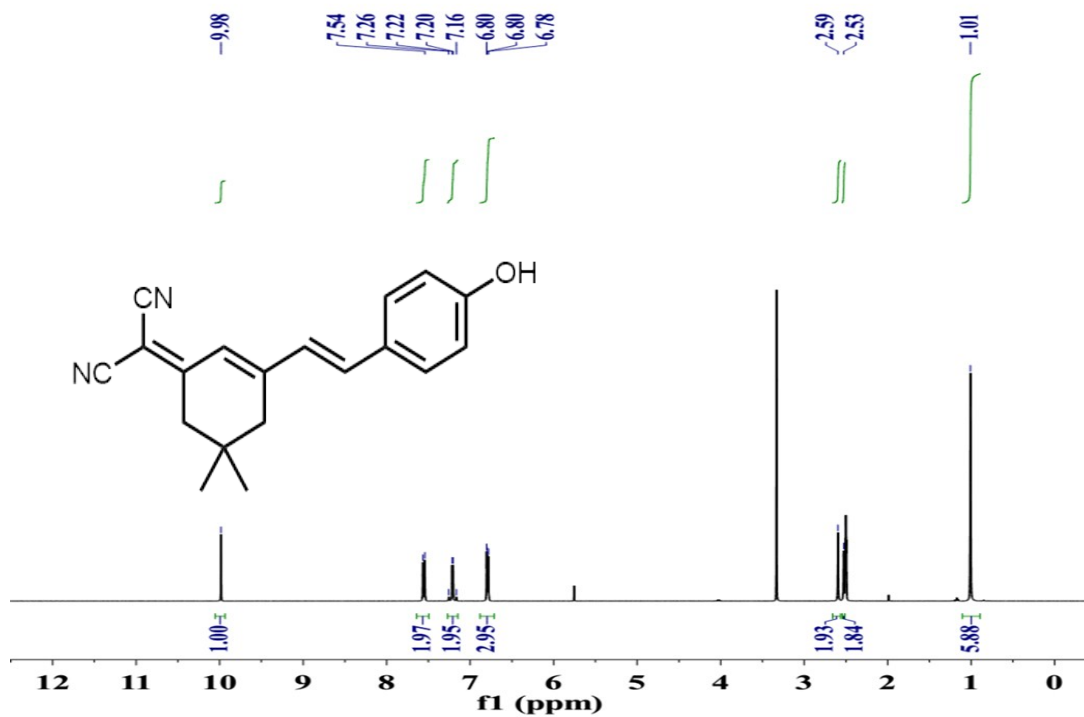


Figure S23. ¹H NMR spectra of NDCM-OH in DMSO-d₆

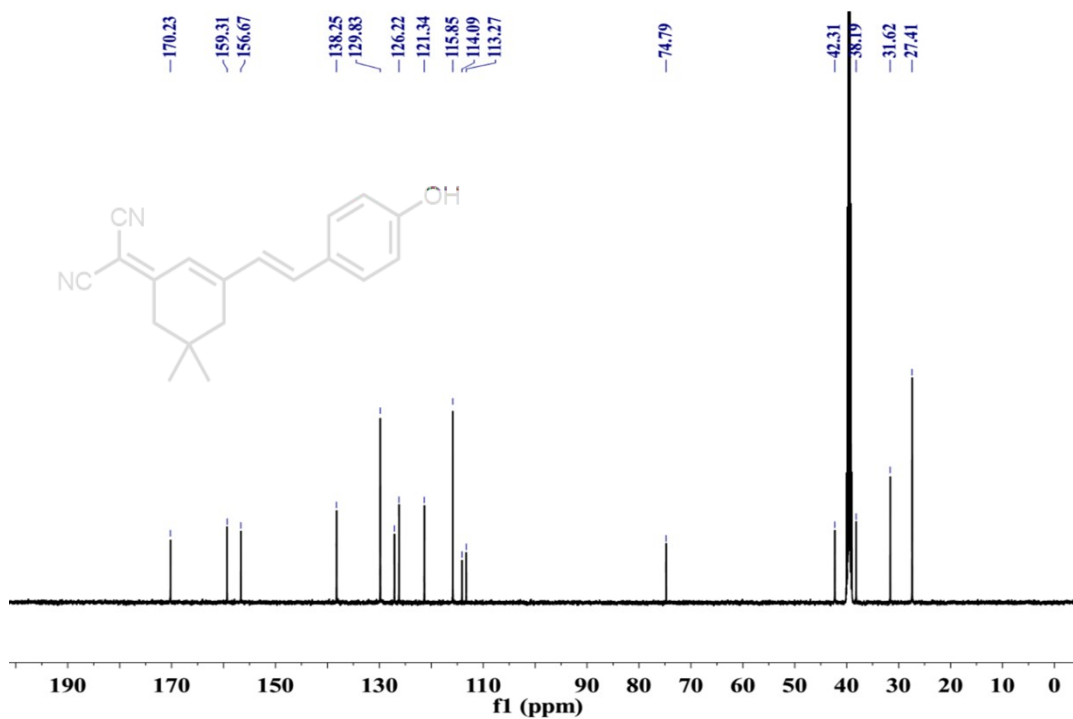


Figure S24. ¹³C NMR spectra of NDCM-OH in DMSO-d₆

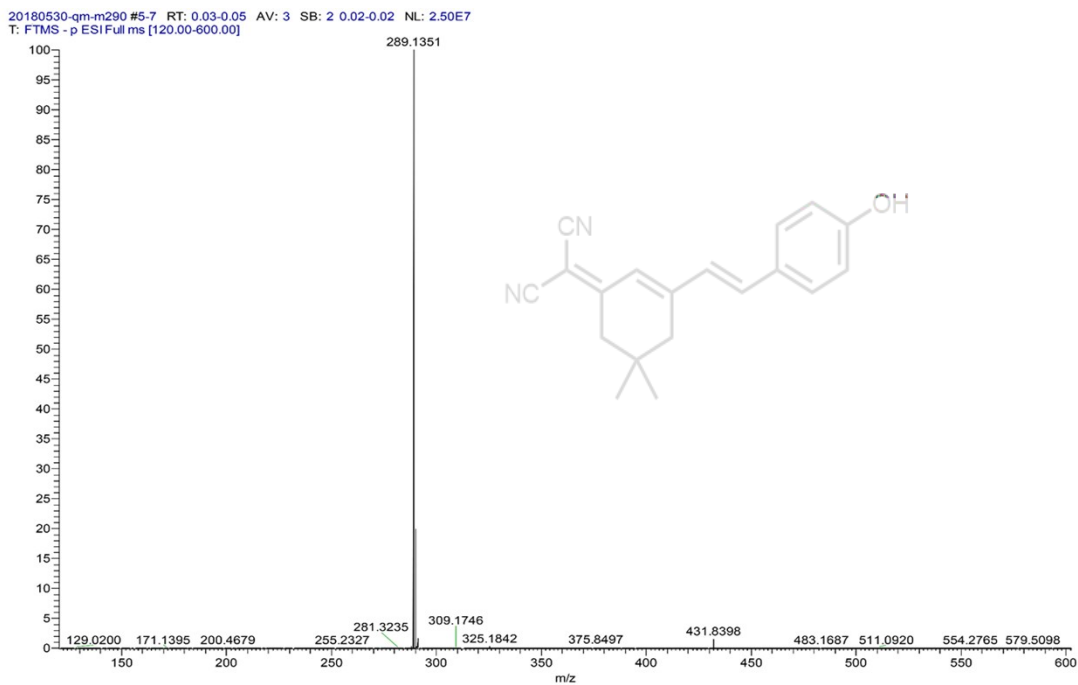


Figure S25. HRMS spectra of NDCM-OH

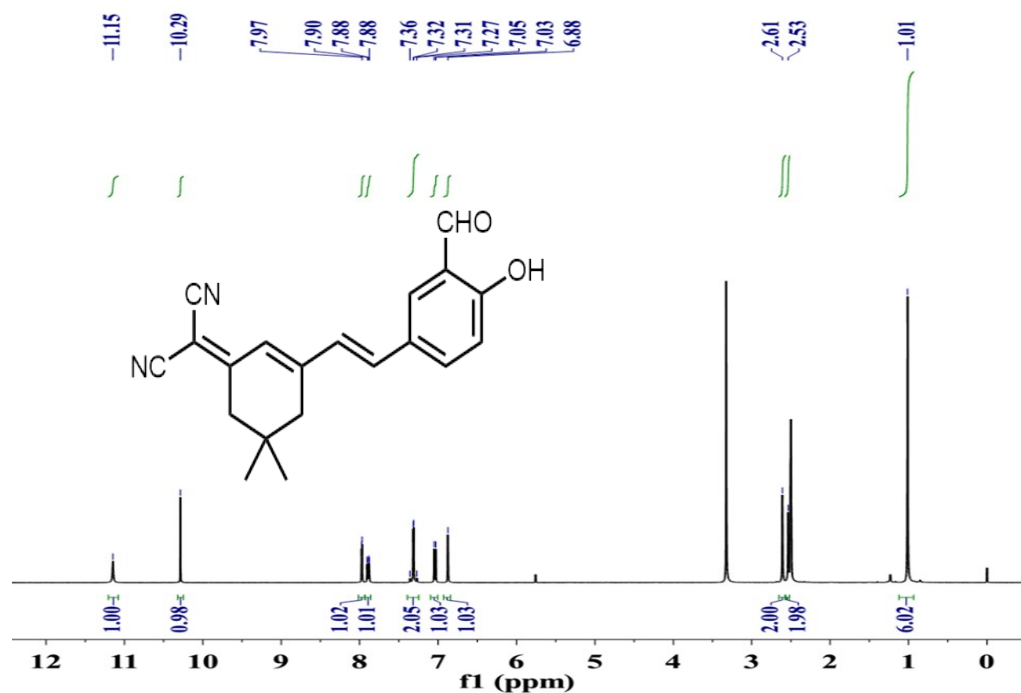


Figure S26. ¹H NMR spectra of NDCM-OH in DMSO-d₆

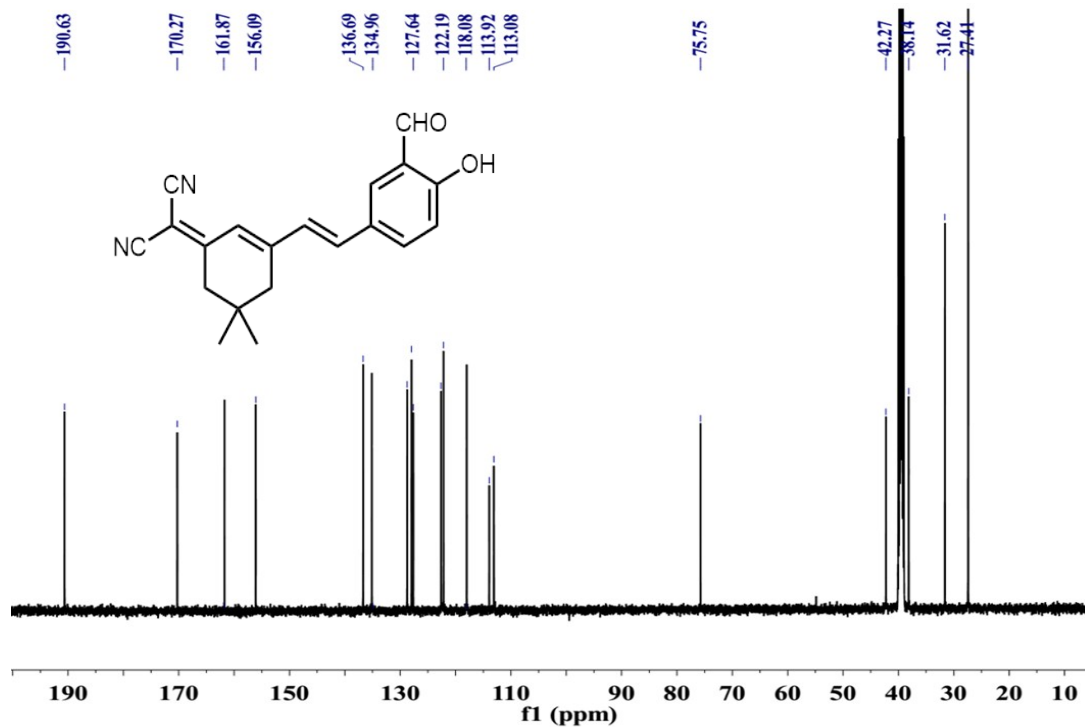
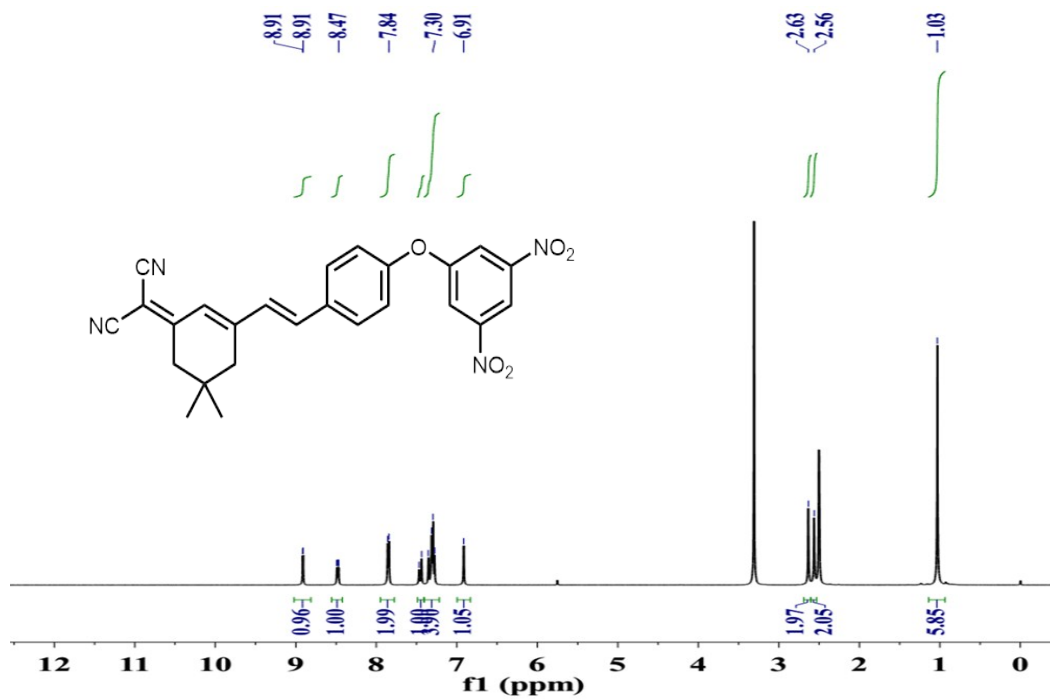
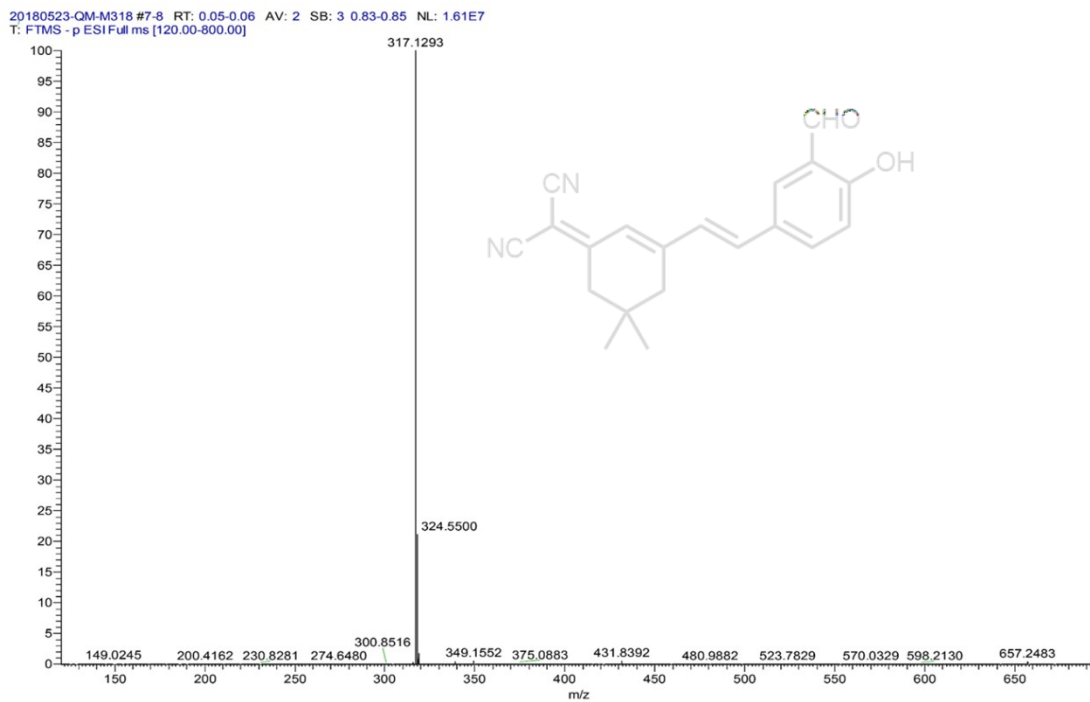


Figure S27. ¹³C NMR spectra of NDCM-CHO-OH in DMSO-d₆



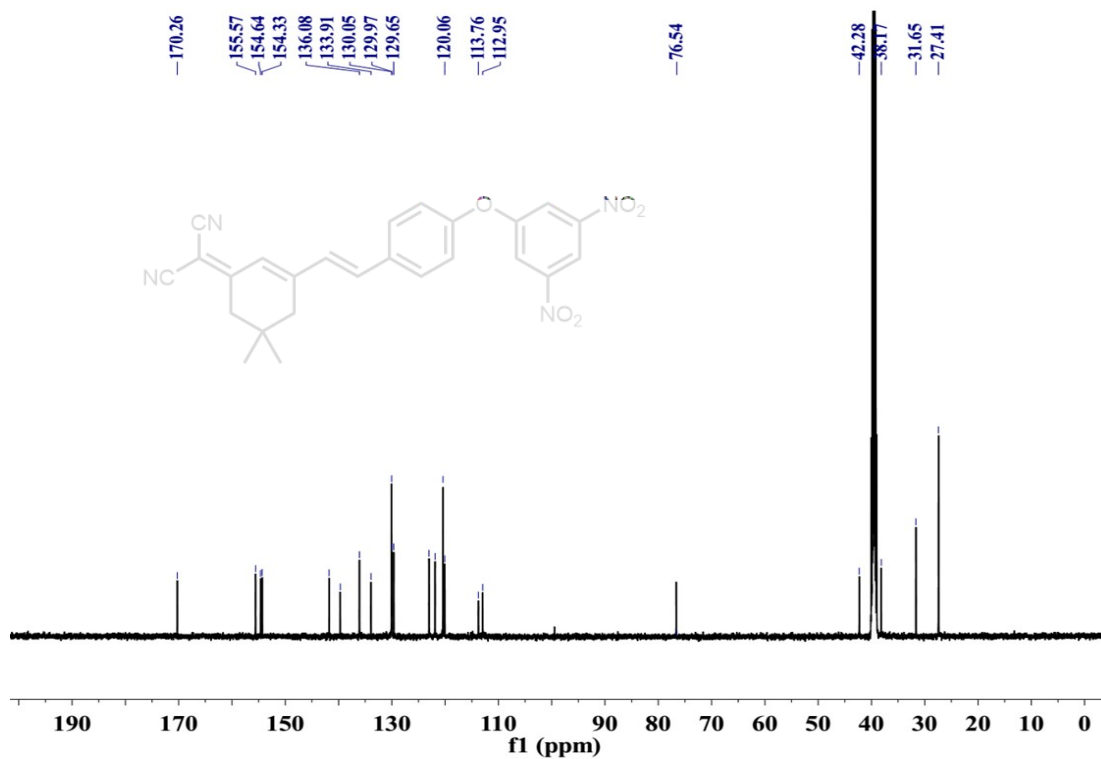


Figure S30. ¹³C NMR spectra of NDCM-1 in DMSO-d₆

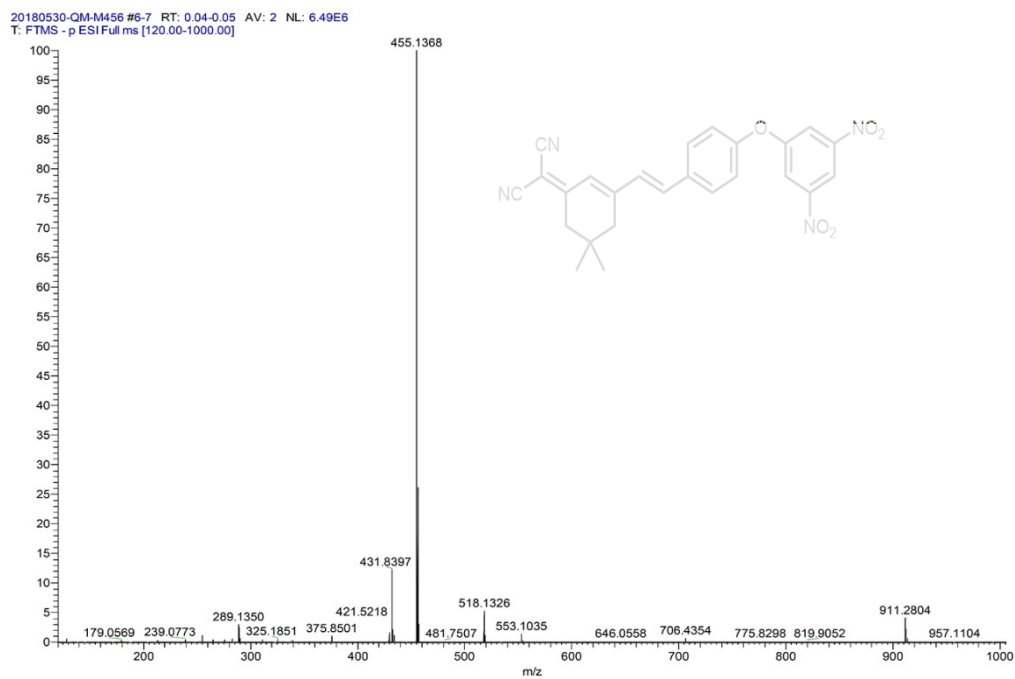


Figure S31. HRMS spectra of NDCM-1

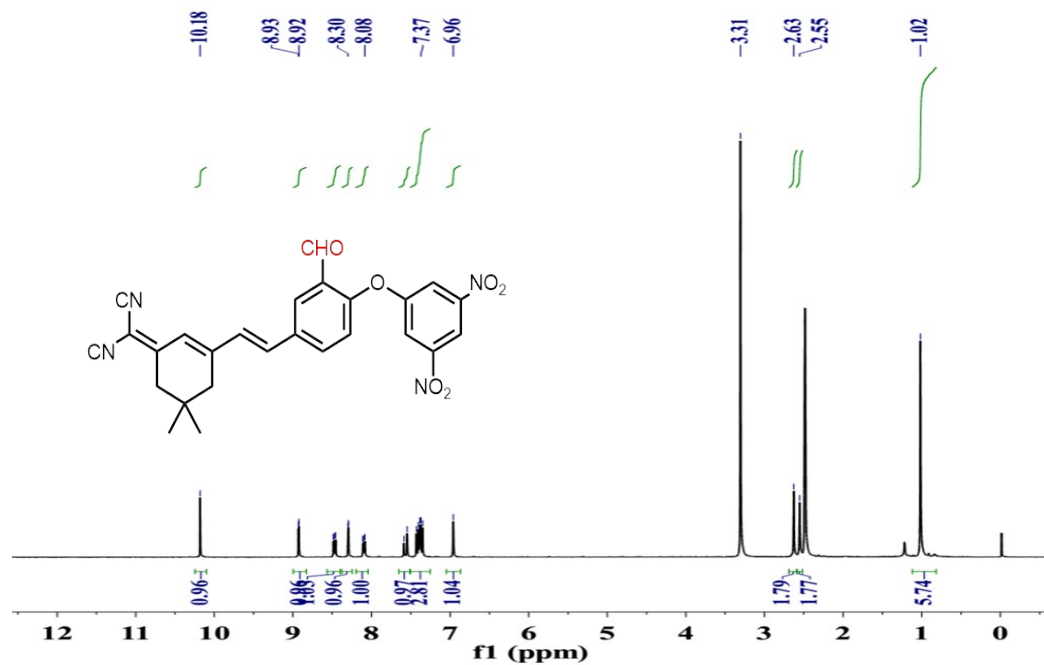


Figure S32. ^1H NMR spectra of NDCM-2 in DMSO-d_6

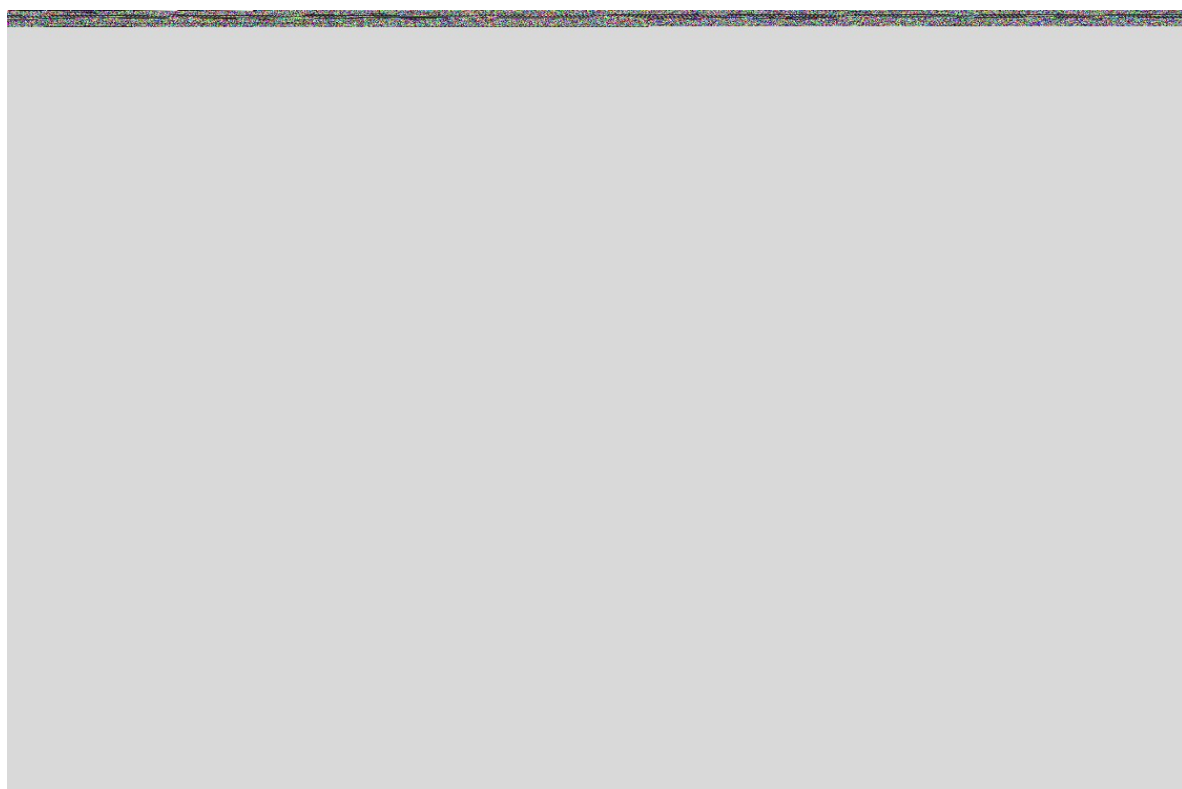


Figure S33. ^{13}C NMR spectra of NDCM-2 in DMSO-d_6

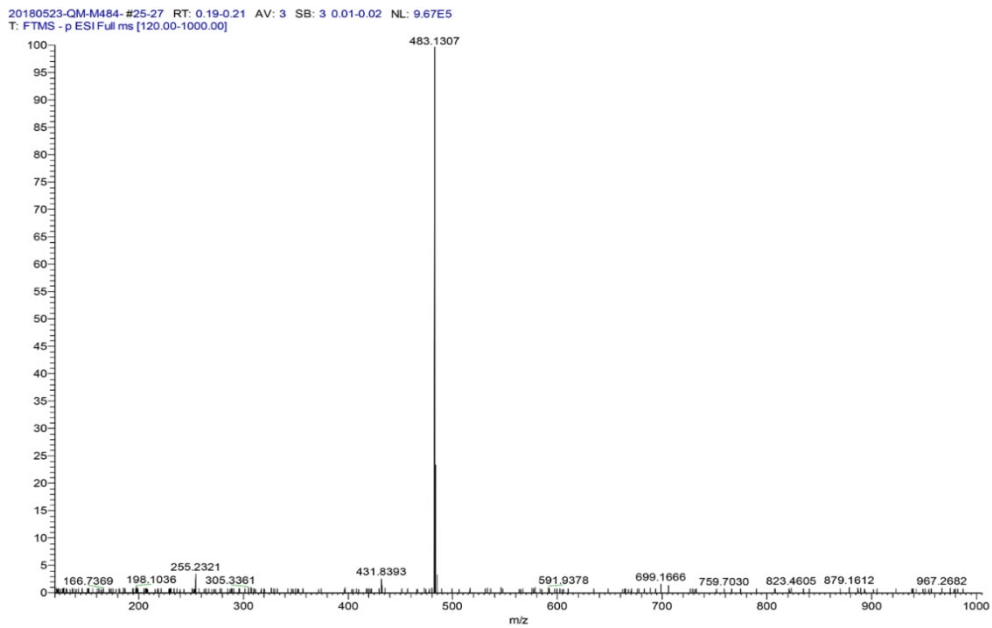


Figure S34. HRMS spectra of NDCM-2